Journal of Energy Storage 73 (2023) 109110

Contents lists available at ScienceDirect

Journal of Energy Storage

journal homepage: www.elsevier.com/locate/est

Research papers

Design, machining and characterization of the components required for the manufacture of a supercapacitor

Jesús M. Rodríguez-Rego [a], Antonio Macías-García [b,*], Laura Mendoza-Cerezo [a], Antonio Díaz-Parralejo [b], Juan Pablo Carrasco-Amador [a]

[a] Department of Graphic Expression, School of Industrial Engineering, Universidad de Extremadura, Avenida de Elvas, s/n, 06006 Badajoz, Spain
[b] Department of Mechanical, Energy and Materials Engineering, School of Industrial Engineering, Universidad de Extremadura, Avenida de Elvas, s/n, 06006 Badajoz, Spain

ARTICLE INFO

Keywords:
Supercapacitors
Electrical conductivity
Carbonaceous materials
Energy storage

ABSTRACT

One of the main European objectives is to promote the change of consumption towards renewable energies, which have shown a remarkable worldwide growth, the problem lies in the fact that the technologies used, which have been developed very rapidly during these years, do not have sufficiently advanced energy storage systems.

The main objectives of this study have been the design and manufacture of supercapacitors that do not suffer corrosion processes and with higher performance.

To this end, supercapacitor connectors have been designed and machined with different materials in order to find the one that best ensures the non-influence of corrosion processes and ensures correct parallelism. In addition, different carbonaceous materials have been tested for the manufacture and subsequent textural, chemical and morphological characterization of the different electrodes and, finally, charge/discharge and cyclic voltammetry tests have been carried out to analyze which parameters are key for the manufacture and improvement of the supercapacitors.

The results showed that the proposed supercapacitor manufacturing methodology is highly recommended to avoid problems derived from poor assembly, reproducibility of results or problems due to the appearance of galvanic couples. Moreover, the electrodes tested showed very interesting results, as demonstrated by the voltammograms, the chronopotentiograms and the specific energy values, the latter showing that the capacitance exerts a notable influence on the energy values, with the PCO1000C/Graphite and PCO1000C/rGO samples showing the highest energy values.

1. Introduction

The high demand for electrical energy worldwide, together with the energy dependence on oil and gases, has led to the search for new sources of energy and energy storage. This aspect, together with the environmental problems caused by the consumption of these fossil fuel sources, has increased in recent years the research to exploit renewable energy sources. All this makes it necessary to have energy storage systems that allow to obtain the maximum storage capacity and ensure electricity consumption [1,2]. Batteries, fuel cells, capacitors and supercapacitors are energy storage systems [3].

There are currently many studies showings significant progress in some storage systems, such as the solid oxide fuel cell (SOFD), which has high efficiency with zero emissions of carbides and sulfides, and dual graphite batteries [4–6]. The problem with these energy storage systems stems from manufacturing difficulties, complications in transferring these devices to the market and problems with performance and durability in industrial environments, resulting in a significant increase in the final cost.

On the other hand, supercapacitors, also known as electrochemical capacitors, are of great importance for the industry because they are a real alternative to batteries due to the advantages they present [7,8]:

- High power output
- Stability after long cycles of use
- Instantaneous charge and discharge
- Reduced dimensions and weight

* Corresponding author.
E-mail address: amacgar@unex.es (A. Macías-García).

https://doi.org/10.1016/j.est.2023.109110
Received 6 June 2023; Received in revised form 10 September 2023; Accepted 27 September 2023
Available online 1 October 2023

In addition, the potential of supercapacitors is very broad as they can store large amounts of energy above other technologies and present multiple possible combinations for their manufacture, making them technologically attractive for many applications and industries such as telecommunications, vehicles or solar.

Supercapacitors are based on electrochemical processes and consist of an electrolyte, two electrodes (anode and cathode) and a porous separator that prevents electronic contact between the conductive materials [9,10]. The electrolyte must have high ionic conductivity and low electrical conductivity so that electrons are forced to circulate around the outside of the device, thus providing the desired energy. In the case of electrodes the ionic and electronic conductivities must be high. The materials used in electrodes are: carbon, transition metal oxides or conductive polymers and the electrolytes can be organic or ionic liquid.

The carbonaceous materials used in the manufacture of supercapacitors have large surface areas, high electrical conductivity, low cost and high chemical stability [11]. These characteristics have been found in materials such as graphene, graphite and activated carbons.

The objectives of this work are, on the one hand, to develop connectors that do not suffer corrosion processes, maintain parallelism, a greater number of contact points, between the connector and the electrode. On the other hand, to fabricate electrodes of carbonaceous materials based on reduced graphene oxide, graphite and activated carbon and to test them in supercapacitors.

2. Materials and methods

The materials used for the development of this work have been the following:

- ➢ Commercial charcoal PCO1000C, supplied by GalaQuim.
- ➢ Natural graphite, supplied by Merck.
- ➢ Reduced graphene oxide (rGO), supplied by Abalonix.
- ➢ PVDF due to its remarkable electrical conductivity and ability to agglomerate carbonaceous materials.
- ➢ Teflon, polytetrafluoroethylene as polymer binder.

These materials have been selected for the conductivity study, with the aim of verifying how the results are affected depending on the allotropic form of carbon and the number of aggregates formed according to their structure.

To carry out this study it was necessary to model and machine a connector from a material that does not suffer aggressive oxidation processes or galvanic couples. For this reason, and after testing copper, which gave poor results, we chose to manufacture in graphite (Figs. 1 and 2).

The starting materials were texturally characterized by N_2 adsorption at 77 K and mercury porosimetry using an Autosorb-1, Quantachrome and an Autoscan-60, respectively. The 77 K N_2 adsorption technique allows determining the specific surface area and the volume of micropores and narrow mesopores, while mercury porosimetry determines the volume of wide mesopores and macropores.

Before performing the electrochemical tests, it is necessary to prepare the electrodes and assemble the cells to be characterized (Fig. 3).

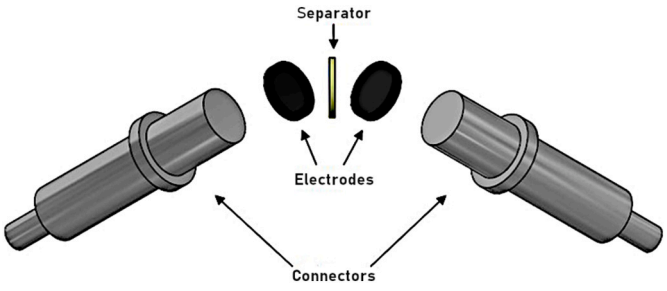

Fig. 1. Components of a supercapacitor.

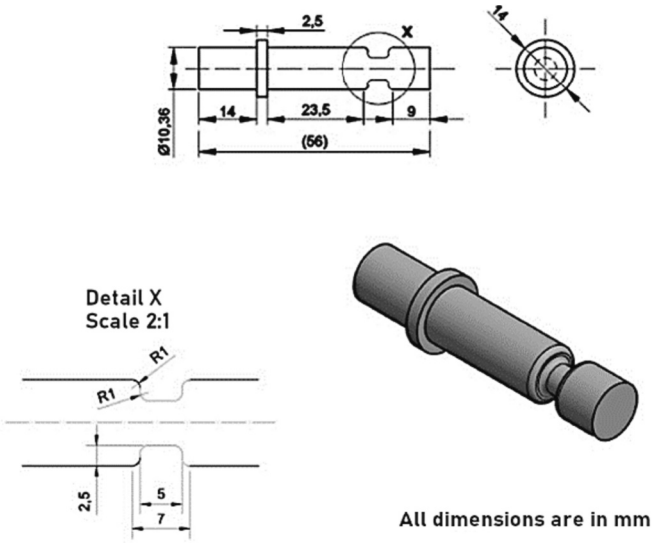

Fig. 2. Graphite connector.

The electrodes have been prepared from different allotropic forms of carbon using reduced graphene oxide (rGO), graphite and commercial activated carbon PCO1000C. As binding agents, PVDF has been used, due to its remarkable electrical conductivity, in addition to polytetrafluoroethylene as a polymer binder. Both the sample components and their proportions are shown in Table 1.

Once the proportions of the different materials that make up the electrode were determined, the carbonaceous materials were ground in an agate mortar. These ground materials are mixed with the polytetrafluoroethylene in a beaker and ethanol is added until the mixture is covered. This mixture is heated 100 °C and at an appropriate rate (more than 200 rpm) so that everything is properly mixed and the ethanol evaporates (boiling point≈78.37 °C), until the mixture becomes a paste and is brought to a glass surface. Using a pipette, ethanol is added to it in small quantities and worked over the whole with a spatula until a homogeneous mass is obtained. Then, with a glass rolling pin, the dough is kneaded until a thin, lump-free layer is obtained. Subsequently, with a 7 mm diameter punch, we obtain the circular electrodes. Finally, the electrodes are placed between two sample holders and placed in an oven at 100 °C for at least 12 h.

The manufactured electrodes were characterized by determining

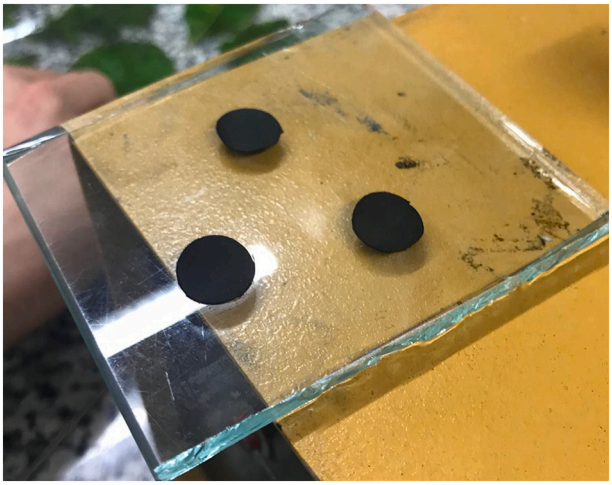

Fig. 3. Electrodes after kneading and before baking.

Table 1
Electrode composition.

Samples	Coal	Additive	PTFE	PVDF
PCO1000C / Graphite	80 % PCO1000C	5 % Graphite	5 %	10 %
Graphite / PCO1000C	80 % Graphite	5 %PCO1000C	5 %	10 %
PCO1000C / rGO	80 % PCO1000C	5 % rGO	5 %	10 %
rGO / PCO1000C	80 % rGO	5 %PCO1000C	5 %	10 %

their electrical conductivity. For this purpose, their electrical conductivity was determined using a hollow cylinder with two copper connectors where the electrode was placed and incorporated into our patented equipment (P202130647).

A 1 M solution of sulfuric acid was used as electrolyte.

A glass microfiber filter supplied by the company MFV2 was used as a separator element because it is semi-permeable. This filter has been cut to the size of the electrodes, ensuring that there is no contact between them and with the function of allowing the ions to pass through.

To manufacture the collectors in this work, graphite collectors (conductive material that withstands electrolyte corrosion well) have been designed and produced in order to test the difference between the charging and discharging speed of the supercapacitor.

The types of supercapacitor cell configurations can be three-electrode and two-electrode. These cells support the rest of the supercapacitor component inside. The three-electrode configuration is a Swagelok® T-shaped cell (see Fig. 4). It has three electrodes formed by the working electrode (WE), which is the object of study, the counter electrode (CE), which could switch places with WE, and the reference electrode (RE). The potential difference between WE and RE is the potential of the working electrode (Ewe), while the current (I) is the current flowing between WE and CE, as shown in Fig. 4.

The Swagelok® two-electrode type cell (see Fig. 5) is used for the assembly of supercapacitors. In this type of configuration both current (I) and potential (Ewe) are measured between WE and CE and behave as two capacitors in series.

Once the supercapacitors were assembled, the electrochemical tests were carried out in a Metrohm model PGSTA101 Autolab potentiostat-galvanostat. The techniques used in this work were cyclic voltammetry (CV) and galvanostatic charge-discharge. Cyclic voltammetry was used with a three-electrode configuration where one electrode was used as a reference to analyze the electrochemical behavior of the active material at each electrode. Charge-discharge tests were carried out on the complete devices in a two-electrode Swagelok® configuration. From these tests, the specific energy and specific power values of the supercapacitor were determined as follows [10,12,13]:

Specific energy ($W{\cdot}h{\cdot}kg^{-1}$):

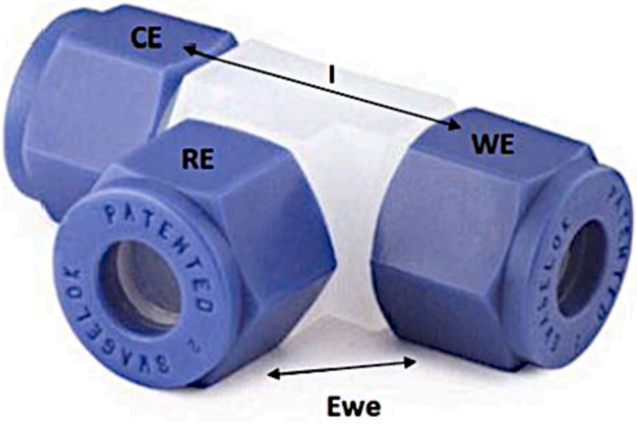

Fig. 4. Swagelok® T three-electrode cell.

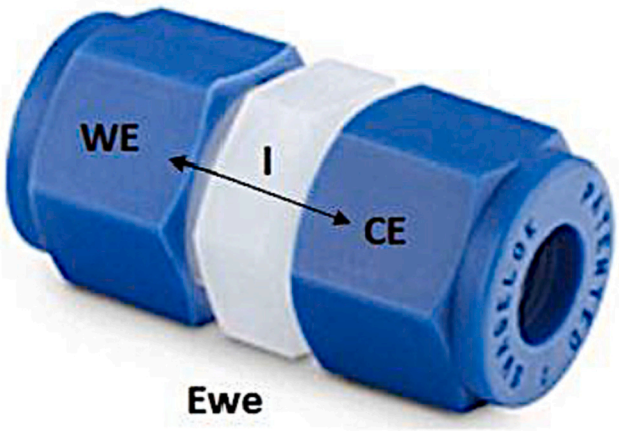

Fig. 5. Swagelok® two-electrode cell.

$$E = \frac{\left(C_{Cell}\cdot V^2\right)\cdot\left(\frac{1000}{3600}\right)}{2} \quad (2.1)$$

Specific power ($W{\cdot}kg^{-1}$):

$$P = \left(V^2\right)/\left(4{\cdot}ESR\right)/\left(mtma/1000\right) \quad (2.2)$$

$$mtma = m- + m+ \quad (2.3)$$

where:

- C_{cell}, Capacity
- V, Potential
- ESR, Equivalent series resistance
- *mtma,* total mass of electrode material

3. Results

Among the materials most commonly used in the manufacture of electrodes for supercapacitors are carbon-based electrodes [14]. These materials are commonly used due to their low cost, easy availability, non-toxic, environmentally friendly and stable [15,16].

The characterization of the porous texture of the carbonaceous starting materials was carried out by means of adsorption isotherms and mercury porosimetry, and the data are shown in Table 2.

The capacitance of a double layer supercapacitor is directly proportional to the surface area of the electrode material. Theoretically, the larger this area the greater the energy storage capacity. However, the situation in practice is more complicated since not all of the surface area is accessible to the electrolyte ions [17]. Therefore, other textural parameters such as pore size distribution must be taken into account and

Table 2
Texture and electrical conductivity data of the carbonaceous materials (conductivity was calculated with 0.15 g of material in a cylindrical sample holder of length 6.69 cm and radius 0.325 cm to which a force of 50 N is applied) (*).

Samples	S_{BET} ($m^2.g^{-1}$)	V_{mi} ($cm^3.g^{-1}$)	V_{me} ($cm^3.g^{-1}$)	$V_{me\text{-}p}$ ($cm^3.g^{-1}$)	$V_{ma\text{-}p}$ ($cm^3.g^{-1}$)	Conductivity ($\Omega^{-1}{\cdot}m^{-1}$)
PCO1000C	1178	0.458	0.402	0.075	0.187	84.19
Graphite	3574	0.003	0.017	11.350	0.751	796.48
rGO	1027	0.402	0.115	0.056	0.581	2.40

(*) Abreviaturas: S_{BET}, specific surface; V_{mi}, micropore volume (reading of adsorbed volume (Vad) at P/P0 = 0,1); V_{me}, mesopore volume (subtraction of V_{mi} from Vad at P/P0 = 0.95); the pore size distribution is represented by Vme-p, mesopore volume and Vma-p, macropore volume (mercury porosiemetry). V_{mi} and V_{me} expressed as liquid volumes.

analyzed in depth. It is important to note the importance of matching the textural properties of the carbon with the dimensions of the electrolyte ions [18,19].

From the study of the data corresponding to the S_{BET} specific surface area, it can be observed that the PCO1000C samples present values similar to those reported in the literature for this type of materials between 500 and 1500 $m^2.g^{-1}$ [20–22].

Reduced graphene oxide rGO has a higher value than those generally reported in the literature for this type of material [23,24].

Graphite has a high S_{BET} specific surface area in excess of 2000 $m^2 \cdot g^{-1}$ which ranks it on a par with superactivated coals [25,26]. This porous development is probably due to its high mesopore volume.

In terms of pore volume, each of these materials presents a well differentiated porous development, which makes their study very interesting. Thus, PCO1000C shows a micro-mesoporous development, while graphite shows a predominance of wide mesopores, probably due to its lamellar structure and rGO a micro-macroporous development.

Once the starting materials had been characterized, the electrodes (see Table 1) and connectors were manufactured. For the manufacture of the graphite connectors, the inventor program was used for their design in order to mechanize the design with a high degree of parallelism, to favor the number of contacts between the connector and the electrode and to give stability to the Swagelok cell components.

Subsequently, the electrodes were texturally characterized and their electrical conductivity was determined. The data obtained are shown in the following table:

From the results of the table, it can be deduced that the most abundant carbonaceous material in the electrode exerts a high influence on the pore volume. Therefore, the samples PCO1000C/graphite and Graphite/PCO1000C are those with a micro-mesoporous and mesoporous distribution, respectively.

The physical characterization of the carbons was evaluated by the electrical conductivity of the electrodes prepared from them. The electrical conductivity of the materials is a very important property to take into account, since it can determine the suitability of an activated carbon as an electrode in a supercapacitor. The higher the conductivity, the greater its contribution to reducing the equivalent resistance of the system, and therefore helps to reduce the power output of the cell.

In electrodes containing graphite, graphite has a very high influence on the conductivity of the electrodes. Graphite has a good electrical conductivity due to the arrangement of the carbon atoms, which form hexagonal rings contained in sheets that are held together by mutual attraction forces. These sheets overlap each other, allowing the migration of electrons, which results in good conductivity.

On the other hand, activated carbons (PCO1000C) are materials that are characterized by their porous structure, which means that the activated carbon conducts electricity to a certain extent.

On the other hand, the low electrical conductivity of rGO is due to the fact that this material supplied to us contained unreduced graphene oxide structures, which hindered the transit of electrons.

When a carbonaceous material is brought into contact with an acidic solution, a charge distribution called an electrochemical double layer develops at the interface. The double layer also influences the adsorption properties of the surface. Therefore, the adsorption isotherm of a body can depend on the applied electric potential. This phenomenon is known as electrosorption.

Once the electrodes were characterized, the supercapacitor was fabricated as described in the previous section.

Electrochemical capacitors based on carbon materials store energy through the formation of the electrical double layer, which is an electrostatic phenomenon that occurs at the electrode-electrolyte interface [19].

Although the formation of the electrical double layer depends on the surface area of the material, other textural parameters such as pore size, pore size distribution or porosity tortuosity are very important as they can limit the accessibility of a given electrolyte [27].

The capacitive properties of the activated carbons were studied by cyclic voltammetry while the performance of the supercapacitors was investigated by galvanostatic charge-discharge cycling.

Fig. 6 shows the cyclic voltammograms of all samples at a sweep rate 0.005 V/s using H_2SO_4 1 M as electrolyte for the four prepared cells.

The carbonaceous systems PCO1000C/Graphite and PCO1000C/rGO showed quasi-rectangular voltammograms typical of electrochemical double layer capacitors (EDL) with low diffusional restriction to the electrolyte. However, a clear difference in the shape of the voltammograms is observed between both systems, so different contributions must be taken into account, thus both samples present a similar microporosity and the mesoporosity more developed in the sample PCO1000C/Graphite. Likewise, the curve corresponding to the PCO1000C/Graphite sample shows a faradic contribution at high and low voltages due to the decomposition of the electrolyte, including some peaks due to redox reactions [28]. The rest of the curves also show a faradic contribution with a very attenuated redox effect.

The absence of a significant amount of functional groups in these carbons (PCO1000C/Graphite and PCO1000C/rGO) explain the quasi-rectangular voltammograms typical of supercapacitors. On the other hand, it is known that the presence of functional groups with groups susceptible to redox processes gives rise to the pseudocapacitance phenomenon [29]. The existence of this phenomenon results in a distortion in the ideally rectangular shape of the cyclic voltammetry.

Table 4 shows the values obtained by cyclic voltammetry. The coulombic efficiency was determined by the charge accumulated in the cathodic and anodic sweeps. The values obtained above 95 % indicate that the electrode behavior is reversible. In view of the previous table, it can be deduced that the samples containing PCO1000C as carbonaceous material in greater proportion (PCO1000C/graphite and PCO1000C/rGO) present a high reversibility against rGO/PCO1000C that slightly reduces this percentage 93 % and rGO/PCO1000C with 57.07 % with a low reversibility probably due to the impurities of the material or to the lack of uniformity in its geometry that presented this type of electrode.

When studying the relationship between the electrical conductivity (Table 3) and the specific capacity (Table 4) of the different electrodes, it is observed that although it is necessary for the electrodes to have electrical conductivity to allow the transit of electrons, there is no quantitative relationship between the two. However, when relating the volume of narrow pores ($V_{mi} + V_{me}$) with the specific capacity, it is observed that the greater the volume of pores, the greater the specific capacity, this is due to the fact that this type of pores facilitates the transit of electrolytes to the surface of the carbonaceous material (Fig. 7).

Swagelok® two-electrode cell enables characterization of supercapacitors by galvanostatic charge-discharge test.

The galvanostatic charging and discharging technique consists of applying a continuous and constant current for a given interval of time until the potential limit set for the charge is reached. In this way, the ions migrate towards the surface of the electrodes and are stored there, at which point the system is said to be charged. However, if at a given moment the applied current is reversed for a period of time, the system will proceed to discharge, releasing energy. The representation of the potential values versus time shows the process of charging and discharging the system. For an ideal capacitor the curve obtained should be perfectly triangular.

As can be seen in Fig. 8, when representing the potential (V) versus time (t), a linear response is obtained with a positive slope when charging the system and with a negative slope when discharging it. Fig. 8 shows that it is also possible to find systems that present an ohmic drop as a consequence of the resistance of the ions to the movement to or from the electrodes and by the mechanism that occurs at the electrode-electrolyte interface.

The obtained chronopotentiograms are shown in Fig. 8, at a current load of 200 mA/g in H_2SO_4 as electrolyte.

Fig. 5 plots the potential (V) versus time (t) and a linear response is

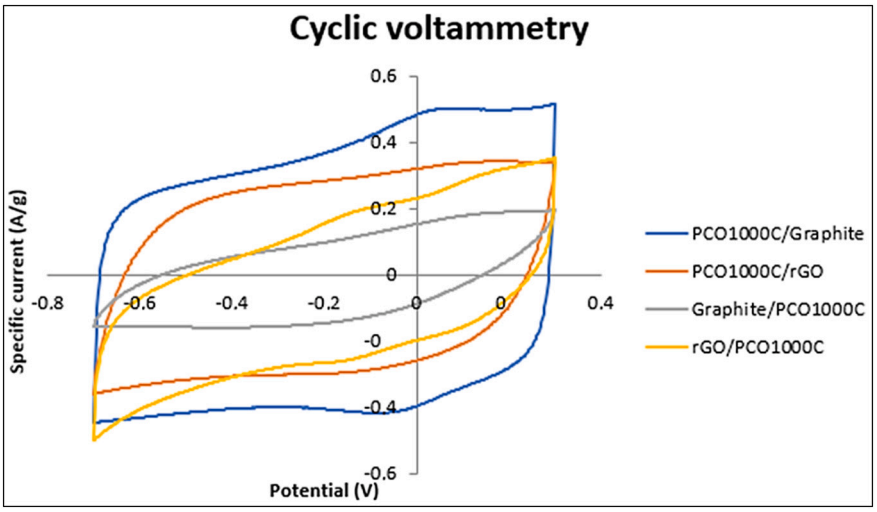

Fig. 6. Cyclic voltammetry in H_2SO_4 at 1 M at 0.005 V/s.

Table 3
Textural and electrical characterization for each electrode.

Samples	S_{BET} ($m^2.g^{-1}$)	V_{mi} ($cm^3.g^{-1}$)	V_{me} ($cm^3.g^{-1}$)	$V_{me\text{-}p}$ ($cm^3.g^{-1}$)	$V_{ma\text{-}p}$ ($cm^3.g^{-1}$)	σ ($\Omega^{-1}.m^1$)
PCO1000C/ Graphite	1121.10	0.367	0.402	0.628	0.187	123.00
PCO1000C/ rGO	993.75	0.386	0.407	0.063	0.179	85.21
Graphite/ PCO1000C	2918.10	0.025	0.039	9.084	0.610	800.96
rGO/ PCO1000C	777.80	0.304	0.106	0.043	0.416	8.26

Table 4
Cyclic voltammetry properties of samples in H_2SO_4 1 M at 0.005 V/s.

Samples	Total electrode mass (g)	Cycle area (A·s)	Specific capacity ($F.g^{-1}$)	Coulombic efficiency μ (%)
PCO1000C/ Graphite	0.017	1.276	75.06	98.3
PCO1000C/ rGO	0.044	2.329	52.81	97.91
Graphite/ PCO1000C	0.014	0.337	22.76	93.17
rGO/ PCO1000C	0.009	0.409	42.67	57,07

obtained with positive slope when charging the system and negative slope when discharging it. Likewise, it is observed that the supercapacitors show almost triangular shapes, which again indicates that the samples behave almost as an ideal electrochemical double layer (EDL) with low resistance and good diffusion of the electrolyte inside the pores, except the sample PCO1000C/rGO associated with a non-ideal behavior (upper peak of the triangle) that presents an ohmic drop consequence of the resistance of the ions to the movement to or from the electrodes and by the mechanism that occurs at the electrode-electrolyte interface. In other words, this behavior is attributable to various contributions associated with the cell configuration (electrolyte resistance, electrode resistance, electrode-connector resistance, etc.).

From the data obtained and represented in Fig. 8 for charging and discharging, the values of specific energy and specific power of the supercapacitor shown in Table 5 were obtained, as indicated in the previous section.

In carbonaceous materials, micropores between 0.7 and 2 nm are characterized by high capacitive performance, however, the maximum capacity of the double layer is obtained with a pore distribution very close to the size of the electrolyte ion [27,30].

Mesopores are important because they are necessary for the efficient transport of ions [31]. Very large or small pores can lead to a decrease in the capacity of the pores [27].

Therefore, the capacitance values shown in Table 5 are in agreement with the porosity values shown in Table 3, where the importance of the micropores and mesopores present in the electrodes is evident.

The capacitance exerts a notable influence on the energy values, as can be seen from Eq. (2.1), with the PCO1000C/Graphite and PCO1000C/rGO samples having the highest energy values.

The equivalent series resistance (ESR) represents the sum of the contact resistance, the charge transfer resistance and the diffusion resistance in the electrolyte pores during the electrochemical process. The equivalent series resistance has a very important influence on the power values as shown in Eq. (2.2). In view of the above table, the sample with the highest power development is PCO1000C/Graphite, which has the lowest ESR. The high power value despite its high ESR of the rGO/PCO1000C sample is striking, probably due to the low value of the mass of its electrodes.

The results show that the electrodes made with PCO1000C/Graphite and PCO1000C/rGO had a capacity and performance in the order or higher than that found in the literature, where the electrodes were made of Ni-doped ZnO, porous carbons using hexamethylenetetramine ($C_6H_{12}N_4$) and $FeCl_3{\cdot}6H_2O$ as raw materials, among other materials [13,32–36] (Table 6).

4. Conclusions

Of the supercapacitor connectors that have been machined (graphite and copper) only the graphite one showed characteristics that allowed it to give good long-term results for the design of a supercapacitor. Copper presented galvanic couples after each use.

Different powdery materials have been characterized texturally, chemically and morphologically. The electrical conductivity of the samples was also determined. It has been determined that textural parameters such as pore size distribution should be taken into account and analyzed in depth to characterize the supercapacitors.

The carbonaceous systems PCO1000C/Graphite and PCO1000C/rGO showed quasi-rectangular voltammograms typical of electrochemical double layer capacitors (EDL).

The chronopotentiograms show that the supercapacitors fabricated

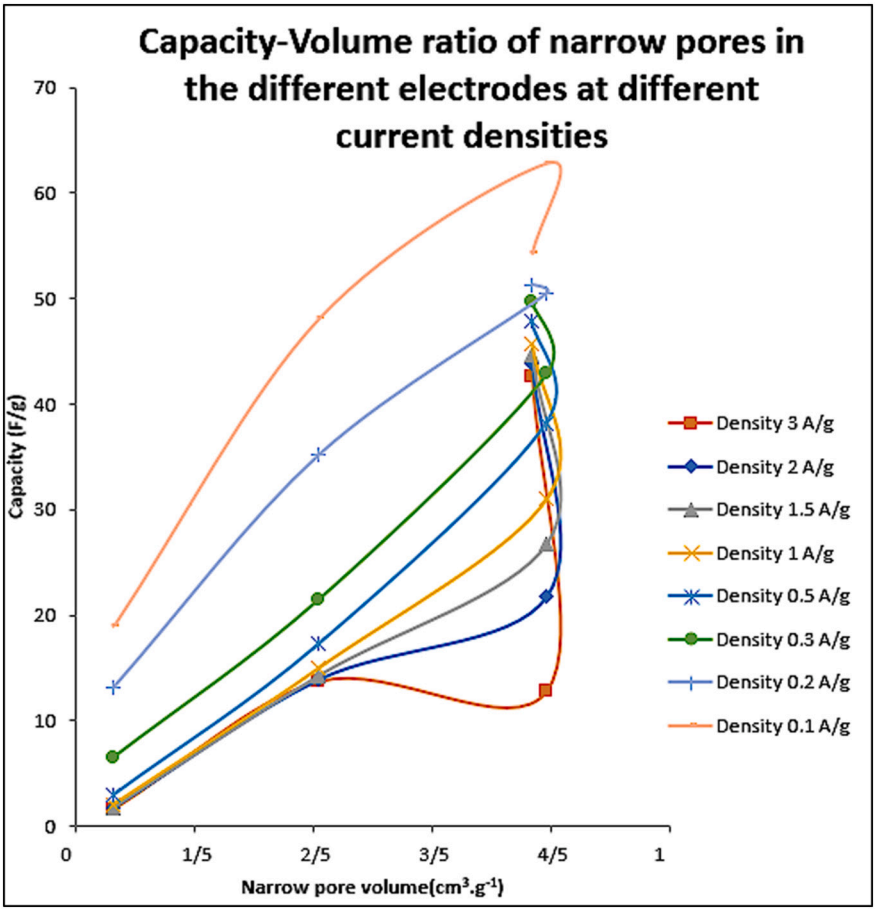

Fig. 7. Narrow electrode pore volume vs. supercapacitor capacity.

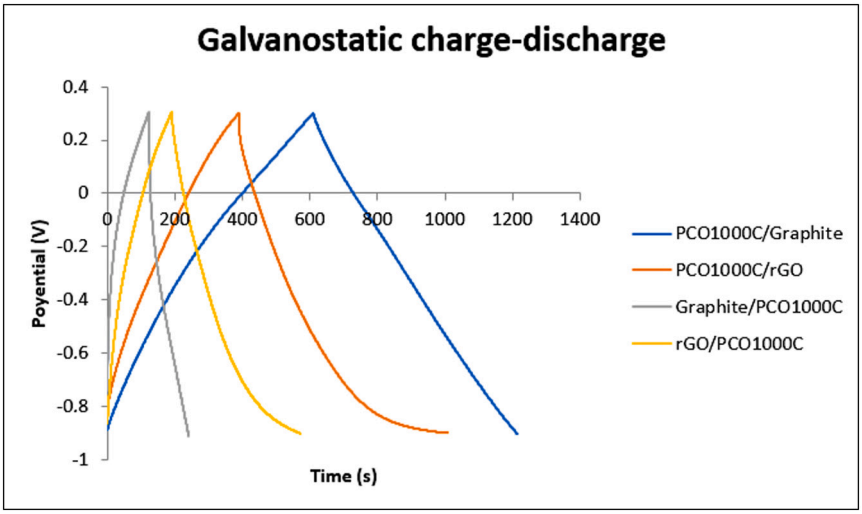

Fig. 8. Galvanostatic charge-discharge in H_2SO_4 at 1 M at 0,005 V/s.

in this study present quasi-triangular shapes, again indicating that the samples behave almost like an ideal electrochemical double layer (EDL) with low resistance and good diffusion of the electrolyte inside the pores, except for sample PCO1000C/rGO which has presented a characteristic shape associated with non-ideal behavior.

The specific energy values show that the capacitance exerts a remarkable influence on the energy values, with samples PCO1000C/Graphite and PCO1000C/rGO having the highest energy values.

In view of the porosity, it can be deduced that, although the pore volume has a considerable influence, since it allows a greater contact between the carbonaceous material and the electrolyte; other factors such as electrical conductivity and the presence of graphitic structures, which seem to exert a greater influence on the values of the capacitance, should not be forgotten.

Table 5
Energy and power values for galvanostatic charge-discharge processes of samples in H_2SO_4 1 M at 200 mA between −0.9 and 0.3 V.

Samples	Supercapacitor capacity ($F{\cdot}g^{-1}$)	Individual electrode capacity ($F{\cdot}g^{-1}$)	Equivalent series resistance ESR (Ω)	Energy ($W{\cdot}h{\cdot}kg^{-1}$)	Power ($W{\cdot}kg^{-1}$)
PCO1000C/ Graphite	51.35	205.40	2.48	0.64	534.25
PCO1000C/rGO	50.55	202.20	8.12	0.63	62.83
Graphite/ PCO1000C	13.23	52.94	34.76	0.16	43.73
rGO/PCO1000C	35.24	140.97	10.98	0.04	213.40

Table 6
Mass of the active material of the two electrodes.

Samples	Active material mass of the two electrodes (g)
PCO1000C/Graphite	0.0170
PCO1000C/rGO	0.0441
Graphite/PCO1000C	0.0148
rGO/PCO1000C	0.0096

CRediT authorship contribution statement

Jesús M. Rodríguez-Rego: Investigation and Writing – Original Draft.
Laura Mendoza-Cerezo: Investigation.
Juan Pablo Carrasco-Amador: Supervision and validation.
Antonio Díaz-Parralejo: Conceptualization.
A. Macías-García: Review & Editing.

Declaration of competing interest

The authors declare that they have no known competing financial interests or personal relationships that could have appeared to influence the work reported in this paper.

Data availability

The raw/processed data required to reproduce these findings cannot be shared at this time as the data also forms part of an ongoing study.

Acknowledgments

The authors are supported by Junta de Extremadura and “FEDER A way of making Europe”, through the Project GR21068.

References

[1] J.K. Kaldellis, D. Zafirakis, Optimum energy storage techniques for the improvement of renewable energy sources-based electricity generation economic efficiency, Energy 32 (12) (2007) 2295–2305, https://doi.org/10.1016/J.ENERGY.2007.07.009.
[2] R. Baños, F. Manzano-Agugliaro, F.G. Montoya, C. Gil, A. Alcayde, J. Gómez, Optimization methods applied to renewable and sustainable energy: a review, Renew. Sustain. Energy Rev. 15 (4) (May 2011) 1753–1766, https://doi.org/10.1016/J.RSER.2010.12.008.
[3] M. Winter, R.J. Brodd, What are batteries, fuel cells, and supercapacitors? Chem. Rev. 104 (10) (Oct. 2004) 4245–4269, https://doi.org/10.1021/CR020730K/ASSET/IMAGES/MEDIUM/CR020730KE00045.GIF.
[4] D. Chen, Y. Zhu, S. Han, L. Anatoly, M. Andrey, L. Lu, Investigate the effect of a parallel-cylindrical flow field on the solid oxide fuel cell stack performance by 3D multiphysics simulating, J. Energy Storage 60 (Apr. 2023) 106587, https://doi.org/10.1016/J.EST.2022.106587.
[5] R. Ren, F. Lai, X. Lang, L. Li, C. Yao, K. Cai, Efficient sulfur host based on Sn doping to construct Fe2O3 nanospheres with high active interface structure for lithium-sulfur batteries, Appl. Surf. Sci. 613 (Mar. 2023) 156003, https://doi.org/10.1016/J.APSUSC.2022.156003.
[6] X. Zhang, et al., A novel aluminum–graphite dual-ion battery, Adv. Energy Mater. 6 (11) (Jun. 2016) 1502588, https://doi.org/10.1002/AENM.201502588.
[7] W. Raza, et al., Recent advancements in supercapacitor technology, Nano Energy 52 (Oct. 2018) 441–473, https://doi.org/10.1016/J.NANOEN.2018.08.013.
[8] G. Diossa, C.D. Castro, Z. Zapata-Benabithe, G. Quintana, Evaluación de la capacidad de almacenamiento de energía en xerogeles de carbono activados obtenidos a partir lignina, Revista ION 30 (2) (May 2018) 17–30, https://doi.org/10.18273/REVION.V30N2-2017002.
[9] J.S. Lázaro, et al., Energía eléctrica y materiales: baterías recargables, supercondensadores y pilas de combustible, Accessed: Jun. 20, 2022. [Online]. Available: www.energia2012.es.
[10] J.M. Rodríguez-Rego, J.P. Carrasco-Amador, L. Mendoza-Cerezo, A.C. Marcos-Romero, A. Macías-García, Guide for the development and evaluation of supercapacitors with the proposal of a novel design to improve their performance, J. Energy Storage 68 (Sep. 2023) 107816, https://doi.org/10.1016/J.EST.2023.107816.
[11] M. Jayalakshmi, K. Balasubramanian, Simple capacitors to supercapacitors-an overview, Int. J. Electrochem. Sci. 3 (2008) 1196–1217. Accessed: Jun. 20, 2022. [Online]. Available: www.electrochemsci.org.
[12] M. Fukuhara, K. Sugawara, Electric charging/discharging characteristics of super capacitor, using de-alloying and anodic oxidized Ti-Ni-Si amorphous alloy ribbons, Nanoscale Res. Lett. 9 (1) (May 2014) 1–6, https://doi.org/10.1186/1556-276X-9-253/FIGURES/6.
[13] T.K. Das, S. Banerjee, A. Kumar, A.K. Debnath, V. Sudarsan, Electrochemical performance of hydrothermally synthesized N-Doped reduced graphene oxide electrodes for supercapacitor application, 2019, https://doi.org/10.1016/j.solidstatesciences.2019.105952.
[14] H. Wang, Q. Hao, X. Yang, L. Lu, X. Wang, Graphene oxide doped polyaniline for supercapacitors, Electrochem. Commun. 11 (6) (Jun. 2009) 1158–1161, https://doi.org/10.1016/J.ELECOM.2009.03.036.
[15] Q. Zhao, et al., Surface modification and performance enhancement of carbon derived from chromium carbide for supercapacitor applications, J. Electrochem. Soc. 162 (6) (2015) 845–851, https://doi.org/10.1149/2.0331506jes.
[16] Y. Zhang, et al., Progress of electrochemical capacitor electrode materials: a review, Int. J. Hydrogen Energy 34 (11) (Jun. 2009) 4889–4899, https://doi.org/10.1016/J.IJHYDENE.2009.04.005.
[17] T.A. Centeno, F. Stoeckli, The volumetric capacitance of microporous carbons in organic electrolyte, Electrochem. Commun. 16 (1) (Mar. 2012) 34–36, https://doi.org/10.1016/J.ELECOM.2011.12.017.
[18] J. Chmiola, G. Yushin, Y. Gogotsi, C. Portet, P. Simon, P.L. Taberna, Anomalous increase in carbon at pore sizes less than 1 nanometer, Science (1979) 313 (5794) (Sep. 2006) 1760–1763, https://doi.org/10.1126/SCIENCE.1132195/SUPPL_FILE/CHMIOLA.SOM.PDF.
[19] R. Mysyk, E. Raymundo-Piñero, F. Béguin, Saturation of subnanometer pores in an electric double-layer capacitor, Electrochem. Commun. 11 (3) (Mar. 2009) 554–556, https://doi.org/10.1016/J.ELECOM.2008.12.035.
[20] O. Ioannidou, A. Zabaniotou, Agricultural residues as precursors for activated carbon production—a review, Renew. Sustain. Energy Rev. 11 (9) (Dec. 2007) 1966–2005, https://doi.org/10.1016/J.RSER.2006.03.013.
[21] S. Acevedo, L. Giraldo, J.C. Moreno, Caracterización textural y química de carbones activados preparados a partir de cuesco de palma africana (*Elaeis guineensis*) por activación química con CaCl2 y MgCl2, Revista Colombiana de Química 44 (3) (Sep. 2015) 18–24, https://doi.org/10.15446/REV.COLOMB.QUIM.V44N3.55606.
[22] J.M. Rodríguez-Rego, L. Mendoza-Cerezo, A.C. Marcos-Romero, J.P. Carrasco-Amador, A. Macías-García, Study of the influence of the type of pores present in the electrodes on the behaviour of a SWAGELOK-type supercapacitor, J. Energy Storage 68 (Sep. 2023) 107670, https://doi.org/10.1016/J.EST.2023.107670.
[23] B. Zhao, et al., Supercapacitor performances of thermally reduced graphene oxide, J. Power Sources 198 (Jan. 2012) 423–427, https://doi.org/10.1016/J.JPOWSOUR.2011.09.074.
[24] A. Alazmi, O. el Tall, S. Rasul, M.N. Hedhili, S.P. Patole, P.M.F.J. Costa, A process to enhance the specific surface area and capacitance of hydrothermally reduced graphene oxide, Nanoscale 8 (41) (Oct. 2016) 17782–17787, https://doi.org/10.1039/C6NR04426C.
[25] J.M.D. Tascón, Novel Carbon Adsorbents, Elsevier Sciences, London, United Kingdom, 2012. Accessed: Jun. 20, 2022. [Online]. Available: https://vdoc.pub/documents/adsorption-by-carbons-novel-carbon-adsorbents-53bsna0sukg0.
[26] J. Rouquerol, F. Rouquerol, P. Llewellyn, G. Maurin, K.S.W. Sing, Adsorption by Powders and Porous Solids: Principles, Methodology and Applications, 2nd ed., Academic Press, 2013 https://doi.org/10.1016/C2010-0-66232-8.
[27] C. Largeot, C. Portet, J. Chmiola, P.L. Taberna, Y. Gogotsi, P. Simon, Relation between the ion size and pore size for an electric double-layer capacitor, J. Am. Chem. Soc. 130 (9) (Mar. 2008) 2730–2731, https://doi.org/10.1021/JA7106178/SUPPL_FILE/JA7106178-FILE003.PDF.
[28] A.J. Bard, L.R. Faulkner, Electrochemical Methods: Fundamentals and Applications, 2nd ed., John Wiley & Sons, INC., 2001.
[29] P. Simon, Y. Gogotsi, Materials for electrochemical capacitors, Nat. Mater. 7 (11) (Nov. 2008) 845–854, https://doi.org/10.1038/nmat2297.
[30] A. Halama, B. Szubzda, G. Pasciak, Carbon aerogels as electrode material for electrical double layer supercapacitors—synthesis and properties, Electrochim.

Acta 55 (25) (Oct. 2010) 7501–7505, https://doi.org/10.1016/J.ELECTACTA.2010.03.040.
[31] H. Shi, Activated carbons and double layer capacitance, Electrochim. Acta 41 (10) (Jun. 1996) 1633–1639, https://doi.org/10.1016/0013-4686(95)00416-5.
[32] M. Wu, et al., Synthesis of Starch-Derived Mesoporous Carbon for Electric Double Layer Capacitor, 2014, https://doi.org/10.1016/j.cej.2014.02.023.
[33] H. Liu, D.D. Zhai, M. Wang, J.S. Liu, X.Y. Chen, Z.J. Zhang, Urea-modified phenol-formaldehyde resins for the template-assisted synthesis of nitrogen-doped carbon Nanosheets as electrode material for supercapacitors, ChemElectroChem 6 (3) (Feb. 2019) 885–891, https://doi.org/10.1002/CELC.201801855.
[34] H. Wei, et al., Advanced Porous Hierarchical Activated Carbon Derived from Agricultural Wastes toward High Performance Supercapacitors, 2019, https://doi.org/10.1016/j.jallcom.2019.153111.
[35] Y. Wang, et al., Ball milling-assisted synthesis and electrochemical performance of porous carbon with controlled morphology and graphitization degree for supercapacitors, J. Energy Storage 38 (Jun. 2021) 102496, https://doi.org/10.1016/J.EST.2021.102496.
[36] I. Neelakanta Reddy, et al., Structural, optical, and bifunctional applications: supercapacitor and photoelectrochemical water splitting of Ni-doped ZnO nanostructures, J. Electroanal. Chem. 828 (Nov. 2018) 124–136, https://doi.org/10.1016/J.JELECHEM.2018.09.048.